

This document is confidential and is proprietary to the American Chemical Society and its authors. Do not copy or disclose without written permission. If you have received this item in error, notify the sender and delete all copies.

**Sequence Independent Cloning and Post-translational
Modification of Repetitive Protein Polymers through Sortase
and Sfp-mediated Enzymatic Ligation**

Journal:	<i>Biomacromolecules</i>
Manuscript ID	bm-2015-01726r.R1
Manuscript Type:	Article
Date Submitted by the Author:	25-Feb-2016
Complete List of Authors:	Ott, Wolfgang; Ludwig-Maximilians-Universitat Munchen Nicolaus, Thomas; Ludwig-Maximilians-Universitat Munchen Gaub, Hermann; LMU, Nash, Michael; Ludwig-Maximilians-University of Munich, Physik

SCHOLARONE™
Manuscripts

1
2
3
4
5
6
7 1 Sequence Independent Cloning and Post-
8
9
10
11 2 translational Modification of Repetitive Protein
12
13
14
15 3 Polymers through Sortase and Sfp-mediated
16
17
18
19
20 4 Enzymatic Ligation
21
22
23
24

25 5 *Wolfgang Ott^{†,‡,§}, Thomas Nicolaus^{†,‡}, Hermann E. Gaub^{†,‡}, and Michael A. Nash^{†,‡,⊥,¶,*}*
26
27
28

29 6 [†]Lehrstuhl für Angewandte Physik, Ludwig-Maximilians-Universität München, 80799 Munich,
30
31 7 Germany.
32

33 8 [‡]Center for Nanoscience (CeNS), Ludwig-Maximilians-Universität München, 80799 Munich,
34
35 9 Germany.
36
37

38 10 [§]Center for Integrated Protein Science Munich (CIPSM), Ludwig-Maximilians-Universität
39
40 11 München, 81377 Munich, Germany.
41
42

43 12 [⊥]Department of Chemistry, University of Basel, 4056 Basel, Switzerland.
44
45

46 13 [¶]Department of Biosystems Science and Engineering, Eidgenössische Technische Hochschule
47 14 (ETH-Zürich), 4058 Basel, Switzerland.
48
49 15

50
51 16 Keywords: Golden Gate assembly, elastin-like polypeptides, sequence independent cloning,
52
53 17 post-translational protein ligation, bioconjugation
54
55

56
57 18 ABSTRACT
58
59
60

1
2
3 19 Repetitive protein-based polymers are important for many applications in biotechnology and
4
5
6 20 biomaterials development. Here we describe the sequential additive ligation of highly repetitive
7
8 21 DNA sequences, their assembly into genes encoding protein-polymers with precisely tunable
9
10 22 lengths and compositions, and their end-specific post-translational modification with organic
11
12 23 dyes and fluorescent protein domains. Our new Golden Gate-based cloning approach relies on
13
14 24 incorporation of only type IIS *BsaI* restriction enzyme recognition sites using PCR, which
15
16 25 allowed us to install ybbR-peptide tags, Sortase c-tags, and cysteine residues onto either end of
17
18 26 the repetitive gene polymers without leaving any cloning scars. The assembled genes were
19
20 27 expressed in *Escherichia coli* and purified using inverse transition cycling (ITC).
21
22 28 Characterization by cloud point spectrophotometry, and denaturing polyacrylamide gel
23
24 29 electrophoresis with fluorescence detection confirmed successful phosphopantetheinyl
25
26 30 transferase (Sfp)-mediated post-translational N-terminal labeling of the protein-polymers with a
27
28 31 Coenzyme A-647 dye (CoA-647), and simultaneous Sortase-mediated C-terminal labeling with a
29
30 32 GFP domain containing an N-terminal GG-motif in a one pot reaction. In a further
31
32 33 demonstration, we installed an N-terminal cysteine residue into a 60 pentapeptide ELP that was
33
34 34 subsequently conjugated to a single chain poly(ethylene glycol)-maleimide (PEG-maleimide)
35
36 35 synthetic polymer, noticeably shifting the ELP cloud point. The ability to straightforwardly
37
38 36 assemble repetitive DNA sequences encoding ELPs of precisely tunable length, and to post-
39
40 37 translationally modify them specifically at the N- and C- termini provides a versatile platform for
41
42 38 the design and production of multi-functional smart protein-polymeric materials.
43
44
45
46
47
48
49
50
51
52 39
53
54 40 INTRODUCTION
55
56
57
58
59
60

1
2
3 41 Repetitive polymers of controlled length and tunable phase-transition behavior are urgently
4
5 42 needed for a variety of applications in the nano/biosciences, including drug delivery^{1,2}, and
6
7 43 medical diagnostics³. Such stimuli-responsive polymeric materials are of high interest for
8
9 44 fundamental investigations into biomolecules under the influence of mechanical, thermal, and
10
11 45 chemical denaturants using biophysical methods such as single-molecule AFM force
12
13 46 spectroscopy^{4,5} and microscale thermophoresis⁶. Elastin like polypeptides (ELPs) are artificial
14
15 47 proteins derived from naturally occurring elastomeric proteins^{7,8}. Recombinant ELPs consist of
16
17 48 repeats of the amino acid sequence Val-Pro-Gly-Xaa-Gly, where Xaa represents any amino acid
18
19 49 except proline. ELPs exhibit a reversible lower critical solution temperature (LCST), and
20
21 50 undergo a phase transition that can be triggered by temperature⁹. Other environmental stimuli
22
23 51 like pH or ionic strength can also be used to collapse ELPs under isothermal conditions. The
24
25 52 guest residue (Xaa) can be used to influence the pH/thermal phase transition properties of the
26
27 53 resulting protein-polymers. Insertion of acidic residues such as glutamate or aspartate in the
28
29 54 guest residue position results in pH-responsive behavior. The transition temperature is strongly
30
31 55 dependent on the concentration and molecular weight, with longer ELP sequences collapsing at
32
33 56 lower temperatures. One can also tune the cloud point by changing several environmental
34
35 57 parameters at once (e.g., temperature, pH, salt), thereby shifting the transition to lower or higher
36
37 58 temperatures as desired¹⁰.
38
39
40
41
42
43
44
45
46
47

48 60 These unique properties of ELPs make them attractive for a variety of applications and scientific
49
50 61 investigations¹¹. Chromatography free protein purification, for example, can be performed by
51
52 62 producing a target protein as an ELP fusion, and precipitating it from cellular extracts, avoiding
53
54 63 the need for affinity tags. This method allows for purification of recombinant proteins under mild
55
56
57
58
59
60

1
2
3 64 conditions. Moreover, it is reported that in combination with maltose binding proteins, ELPs can
4
5 65 improve the solubility of fusion domains and thereby improve expression yields¹²⁻¹⁴.
6
7
8 66

9
10 67 In the field of biomaterials science, ELPs represent a viable option as a scaffold material for
11
12 68 tissue engineering, or as carriers for drug molecules. Applications for *in vivo* systems demand
13
14 69 high predictability and controllability of the biophysical behavior of the molecules. Since ELPs
15
16 70 consist only of amino acids, they are competitive in terms of biocompatibility and biodegradation
17
18 71 *in vivo* as compared to their synthetic organic polymer counterparts^{15,16}. ELPs possess the added
19
20 72 advantage of complete monodispersity. More fundamentally, the phase transition characteristics
21
22 73 of ELPs have served as an ideal model system for theoretical calculations and modeling
23
24 74 studies¹⁷⁻²¹. Additionally, conjugates between ELPs and synthetic polymers (e.g., PEG) are of
25
26 75 high interest, and would benefit from site-specific conjugation approaches^{22,23}.
27
28
29
30
31 76

32
33 77 In order to fully leverage the versatility of repetitive protein-polymers such as ELPs, modular
34
35 78 and straightforward approaches to cloning and site-specific post-translational modification are
36
37 79 highly desirable. Standard solid-phase gene synthesis methods are so far not able to produce the
38
39 80 long (>600 bp) strands of repetitive DNA required for encoding thermally responsive elastin-like
40
41 81 polypeptides (ELPs) with lengths > 200 amino acids. Typically rationally designed ELPs are
42
43 82 constructed using recursive directional ligation (RDL), which requires plasmid amplification,
44
45 83 and restriction digestion, and imposes certain restrictions (i.e., the absence of restriction sites)²⁴.
46
47 84 Larger ELP genes can also be obtained with the OERCA (overlap extension rolling circle
48
49 85 amplification) method, which generates a distribution of unspecified lengths of repetitive DNA
50
51 86 sequences²⁵.
52
53
54
55
56
57
58
59
60

1
2
3 87
4
5
6 88 Compared to the RDL method our Golden Gate approach presented here avoids cloning scars
7
8 89 due to the use of type IIS restriction enzymes, and is able to cut scarlessly within the coding
9
10 90 region^{24,26}. The PRe-RDL (RDL by plasmid reconstruction) method relies on several type IIS
11
12 91 restriction enzymes and requires certain modifications of the backbone beforehand²⁷.
13
14
15 92

16
17 93 Our method is applicable to a broad spectrum of plasmids, since the only limitation is one type
18
19 94 IIS restriction enzyme with a recognition site not present in the backbone. Along with this
20
21 95 advantage, it is likewise ideal for adding ELPs to an existing gene-containing plasmid to create
22
23 96 fusion proteins with different length ELPs. The combinational possibilities also do not rely on a
24
25 97 plasmid library, but can be designed using a bottom up block assembly approach. Our approach
26
27 98 can also be used in a complimentary way with the existing RDL and OERCA methods, for
28
29 99 example, by easily generating fast and reliable plasmid libraries which can then be further
30
31
32 100 extended by combining with RDL or OERCA methods.
33
34
35

36 101
37
38 102 We present a sequence independent approach based on the Golden Gate technology employing
39
40 103 polymerase chain reaction (PCR) amplification of short ELP repeats and ligation into a plasmid
41
42 104 backbone to produce repetitive ELP genes with specific peptide tag end groups for covalent post-
43
44 105 translational modification. A single type IIS restriction enzyme is used to create unique ends and
45
46 106 guarantee the order of DNA block assembly. Using this method, repetitive DNA sequences up to
47
48 107 hundreds of nm in length (i.e., 120 pentapeptide repeats of ELPs) can be rationally designed and
49
50 108 created. 5' and 3' tags for post-translational modifications were readily incorporated during the
51
52 109 cloning workflow, providing many further possibilities for downstream conjugation and labeling.
53
54
55
56
57
58
59
60

1
2
3 110 Due to the modularity of the system, we were also able to readily install peptide tags (i.e., ybbR²⁸
4
5 111 and Sortase sequences) to the ELP, enabling enzyme-catalyzed ligation of the peptides to
6
7 112 fluorescent proteins and organic dyes (as shown below). Our approach builds on the prior
8
9 113 method shown by Huber *et al.* which demonstrated fusion of different kinds of repetitive DNA to
10
11 114 create chimeras of ELPs, silk peptides and similar proteins²⁹. Our methodology is also
12
13 115 compatible with their approach with the advantage of using only one type IIS restriction enzyme.
14
15
16
17 116
18
19
20 117 Alternatively, it is possible to modify the carrier plasmid in the first amplification round and add
21
22 118 ELP flanking tags or protein domains easily. Since the reaction starts new every three fragments,
23
24 119 one can easily define block patterns that build up an overall sequence. For example, pH
25
26 120 responsive blocks can be interspersed with pH-insensitive blocks. In regards to user-friendliness,
27
28 121 the presented method is advantageous because it relies on the same ELP gene inserts, which can
29
30 122 be reused. Once successful amplification and purification of the sequences is achieved, the PCR
31
32 123 amplicons can be stored and used again as needed. This way it is possible to create a whole
33
34 124 library of gene sequences and, if desired shuffle these each ligation cycle. Post-translational
35
36 125 fusion of ELPs using Sortase ligation circumvents the known issue of low protein yields for N-
37
38 126 terminally located ELP domains in fusion proteins^{30,31}. Instead of optimizing expression
39
40 127 conditions for proteins of low yield, a protein of interest can be produced in its native state and
41
42 128 fused afterwards post-translationally with the ELP domain. To the best of our knowledge, this
43
44 129 represents the first report using a Sortase-based recognition sequence to fuse ELP proteins to
45
46
47
48
49 130 other proteins^{13,32}.
50
51
52
53
54
55
56
57
58
59
60

131 MATERIALS AND METHODS

132 All used reagents were of analytical purity grade and were purchased from Sigma-Aldrich (St.
133 Louis, MO, USA) or Carl Roth GmbH (Karlsruhe, Germany).

134
135 **Monomer Gene Synthesis.** A synthetic gene encoding 150 nucleotides (10 pentapeptide repeats)
136 for the (VPGVG)₅-(VPGAG)₂-(VPGGG)₃ peptide (Centic Biotech, Heidelberg, Germany) served
137 as starting material (see Supporting Information, DNA Sequence 1 and Protein Sequence 1).

138
139 **Cloning.** Golden Gate cloning was employed to create the different rationally designed ELP
140 constructs²⁶. PCR (Backbone: 98°C 2 min, (98°C 7 s, 72°C 2 min 30 s) x30, 72°C 5 min; Insert:
141 98°C 2 min, 98°C 7 s, 60°C 7s, 72°C 5 s) x30, 72°C 5 min) was performed with a Phusion high
142 fidelity polymerase master mix. A typical 20 µl PCR mix contained 10 µl Phusion high fidelity
143 polymerase master mix (Thermo Fisher Scientific Inc., Waltham, MA, USA), 0.5 µl per forward
144 and reverse primer (10 µM), 1.5 µl DMSO, 1 ng of template and water. All primers (biomers.net,
145 Ulm, Germany) used in this study are listed in Tab. 1.

146 **Table 1.** Overview of employed primers

Primer	Sequence 5' – 3'
(1a) FW ELP I ybbR	TATATAGGTCTCCTGGCTGTGCCGGGAGAAGGAGTCCCTGG TGTCGGTGTCCAGGCG
(1b) REV ELP I	GGTCTCCTCCTTCACCCGGAACGCCACCCCCCGGAACACC GCCGC
(2a) FW ELP II	TATATAGGTCTCAAGGAGTACCAGGCGAAGGCGTGCCGG GTGTC
(2b) REV ELP II	ATATATGGTCTCACCCCTCACCCGGAACGCCACCCCCCGGA ACACCGCCGC

1		
2		
3		
4	(3a) FW ELP III	TATATAGGTCTCGAGGGTGTACCAGGCGAAGGGGTGCCGG
5		GTGTC
6		
7	(3b) REV ELP III	ATATATGGTCTCCGGCAGACCTTCACCCGGAACGCCACCCC
8	LPETGG	CCGGAACACCGCCGC
9		
10	(4) REV ELP III	ATATATGGTCTCCACCTTCACCCGGAACGCCACCCCCCGG
11		AACACCGCCGC
12		
13	(5) FW backbone	ATATATGGTCTCCTGCCGGAAACCGGCGGCTAACTCGAGTA
14	LPETGG	AGATCCGGCTGC
15		
16	(6) REV backbone	ATATATGGTCTCAGCCAGTTTAGAAGCGATGAATTCCAG
17	ybbR	
18		
19	(7) FW backbone	GACTCTCTGGAATTCATCGCTTCTAACTGGCTGGTCTCC
20	ybbR	AGGTGTGCCGGA
21		
22		
23	(8) FW ELP II ybbR	TATATAGGTCTCCTGGCGGTACCAGGCGAAGGGGTGCCGG
24		GTGTC
25		
26		TATATAGGTCTCCTGGCGGTACCAGGCGAAGGCGTGCCGG
27	(9) FW ELP III	GTGTC
28	ybbR	
29		GACTCTCTGGAATTCATCGCTTCTAACTGGCTGGTCTCC
30	(10) FW ELP N Cys	TGCGTGCCGGGAGAAGGAG
31		
32	(11) REV backbone	CCCGGCACAGCCAGTTTAGAAGCGATGAATTCCAGAGAG
33		TCGGTCTCACATATGTATATC
34		

35 Primers 1 – 7 are employed for the cloning of the ELPs with 3 fragments growth every cycle.
 36 1-4 are the primers necessary for insert amplification, 5-7 for the amplification of the
 37 backbone. Primers 8 and 9 are only important for ELP cloning procedures with the addition of
 38 one or two fragments. Primers 10 and 11 were used to change the 5' flanking site of the ELP
 39 gene from the gene for the ybbR-tag to a cysteine. DNA Sequence is styled in different ways:
 40 **bold** (annealing region), underlined (*BsaI* recognition site), **highlighted in grey** (*BsaI*
 41 restriction site)
 42
 43
 44

45
 46
 47 147 In the first round of PCR (see backbone PCR above, 55°C 7s annealing), the backbone of a
 48
 49 148 modified pET28a vector (Merck KGaA, Darmstadt, Germany) was linearized. The PCR product
 50
 51 149 contained at the 5' end the sequence for a ybbR-tag (DSLEFIASKLA) and at the 3' end a C-
 52
 53
 54 150 terminal Sortase recognition sequence (LPETGG)^{33,34}. Sequences of all PCR fragments
 55
 56 151 (backbone, ELP I, II, III, IV) and a description for primer design (see Supporting Information,
 57
 58
 59
 60

1
2
3 152 Primer 12) based on an original pET28a vector are attached in the supporting information (Fig.
4
5 153 S1 – S9, DNA Sequence 1-6 and Fig. S14-S18).

6
7
8 154
9
10 155 The superfolder GFP (sfGFP) plasmid was created with Gibson Assembly³⁵. The gene (Addgene
11
12 156 ID: 58708)³⁶ was amplified with overlaps to match a linearized vector containing sequences
13
14
15 157 encoding N-terminal HIS₆-tag, a TEV protease cleavage site and two glycines (compare the PCR
16
17 158 program above; 55°C annealing and an extension time of 1 min. 30 s; see Supporting
18
19 159 Information, DNA Sequence 8 and Protein Sequence 4).

20
21
22 160
23
24 161 All PCR products were digested (37°C, 1 - 12 h) with FD-*DpnI* (Thermo Fisher Scientific Inc.,
25
26 162 Waltham, MA, USA) and purified either with QIAquick PCR purification kit or gel extraction kit
27
28 163 (Qiagen, Hilden, Germany) (Supporting Information, Fig. S10, Fig. S13). *DpnI* was added to
29
30 164 digest the methylated plasmids serving as starting material (template) in the PCRs, to reduce
31
32 165 number of false positive clones in the following transformation.

33
34
35 166
36
37
38 167 Typically, a 25 µl Golden Gate reaction (2.5 µl CutSmart buffer (10x), 1.25 µl T7 ligase, 1.25 µl
39
40 168 *BsaI*-HF and 2.5 µl ATP (10 mM), New England Biolabs, Ipswich, MA, USA) was set up. The
41
42 169 inserts were added in 10-fold molar excess to the backbone (ratio of 0.1 pmol insert to 0.01 pmol
43
44 170 backbone). The reaction was performed in a thermo cycler (25x 37°C 2 min, 25°C 5 min; 37°C
45
46 171 10 min; 80°C 10 min). For the Gibson Assembly reaction, 10 µl of the master mix (2x, New
47
48 172 England Biolabs, Ipswich, MA, USA) were mixed with 0.01 pmol vector and 0.1 pmol insert.
49
50 173 The reaction was incubated for 1 h at 50°C. For the replacement of the ybbR-tag with cysteine,
51
52 174 the PCR linearized product was first digested with *BsaI*-HF together with FD-*DpnI* (1h, 37°C, 5
53
54
55
56
57
58
59
60

1
2
3 175 min, 80°C). The reaction was supplied with 1 µl of dNTPs (10 mM, New England Biolabs,
4
5
6 176 Ipswich, MA, USA), 1 µl of Klenow Fragment (10 U/µL, Thermo Fisher Scientific Inc.,
7
8 177 Waltham, MA, USA), and incubated (37°C, 15 min, and 75°C, 10 min). After a gel extraction,
9
10 178 the corresponding band was excised and a blunt end reaction (6.5 µl PCR product, 1 µl ATP (10
11
12 179 mM), 1 µl CutSmart buffer (10x), 0.5 µl PEG-6000, 1.0 µl T4 Polynucleotide Kinase, 1.0 µl T4
13
14 180 Ligase) was set up (37°C 15 min, 22°C 45 min, 80°C 7 min).

15
16
17 181 In case of the Golden Gate reaction, 10 µl and in case of the Gibson Assembly or the blunt end
18
19 182 ligation 2 µl were used to transform DH5α cells (Life Technologies GmbH, Frankfurt, Germany;
20
21 183 30 min on ice, 42°C 1 min, 1 h 37°C). The transformed culture was plated on appropriate
22
23 184 antibiotic LB-Agar plates. A small number (<10) of clones were analyzed by colony PCR, or
24
25 185 analytical restriction digestion (FD-*EcoRI*, Thermo Fisher Scientific Inc., Waltham, MA, USA)
26
27 186 followed by sequencing (Supporting Information, Tab S1).
28
29
30
31

32 187
33
34 188 **Protein Expression.** For ELP expression, chemically competent *E. coli* NiCo21(DE3) (New
35
36 189 England Biolabs, Ipswich, MA, USA) were transformed with 50 ng plasmid DNA³⁷. The cells
37
38 190 were incubated in kanamycin containing, autoinducing ZYM-5052 media (supplemented with an
39
40 191 amino acid mix 0.1 mg/ml) 24 h at 25°C³⁸⁻⁴⁰. After harvesting, ice cooled cells were lysed using
41
42 192 sonication (Bandelin Sonoplus GM 70, Tip: Bandelin Sonoplus MS 73, Berlin, Germany; 40 %
43
44 193 Power, 30 % Cycle 2x 10 min). The supernatant of the lysate (15000 g, 4°C, 1 h) was heated to
45
46 194 60°C for 30 min to denature most of the *E. coli* host proteins. In a second step, the collapsed
47
48 195 ELPs within this clouded solution were rehydrated by incubating under continuous mixing for 2
49
50 196 h at 4°C. This allowed the resolubilization of the ELPs while the precipitated host proteins
51
52
53 197 remained insoluble. A centrifugation step (15000 g, 4°C, 30 min) was used to separate the
54
55
56
57
58
59
60

1
2
3 198 soluble ELPs and remaining proteins from precipitated cell debris. The clear supernatant turned
4
5 199 immediately cloudy after adding 1 M acetate buffer (final concentration 50 mM, pH 3.5), and 2
6
7
8 200 M NaCl in crystalline form. The mixture was incubated for 30 min at 60°C. The collapsed ELPs
9
10 201 were collected by centrifugation (3220 g, 40°C, 75 min). The obtained pellet was re-solubilized
11
12 202 in 50 mM TRIS-HCl (pH 7.0) and incubated over night at 4°C. The remaining precipitated debris
13
14 203 were removed by a final centrifugation step (3220 g, 4°C, 60 min). The supernatant was mixed
15
16 204 again with acetate buffer and sodium chloride to collapse the ELPs. After the heated incubation
17
18 205 and centrifugation step, the pellet was resolubilized in buffer (50 mM TRIS-HCl, pH 7.0)^{14,41}.
19
20 206 The purity of the ELP was confirmed by SDS-PAGE (Any kD™ Mini-PROTEAN® Stain-
21
22 207 Free™ Gels, Bio-Rad Laboratories GmbH, Hercules, CA, USA), in order to detect any
23
24 208 remaining contaminant host proteins. The ELPs were labeled with CoA-647 (New England
25
26 209 Biolabs (Ipswich, MA, USA) and Sfp (37°C, 1 h, 5 mM MgSO₄) to visualize them. After
27
28 210 labeling, the ELPs were mixed with 6x Loading buffer and heated to 95°C for 10 min⁴². Usually
29
30 211 a purity grade of >95% was obtained. Purity analysis was performed by overlaying the UV active
31
32 212 Stain-Free™ technology from Bio-Rad (labeling all tryptophan side groups of *E. coli* host
33
34 213 proteins) and a fluorophore specific red channel for the CoA-647-ELP constructs (Supporting
35
36 214 Information Fig. S11). MALDI-TOF analysis of ELP samples ELP₃₀₋₅₀ was performed to
37
38 215 increase confidence in the high purity of the samples (Supporting Information, Fig. S19). ELPs
39
40 216 were stored at 4°C in 50 mM TRIS-HCl, pH 7.0.
41
42
43
44
45
46
47
48 217
49
50 218 The final ELP concentration was photometrically determined at 205 nm (Ultrospec 3100 pro,
51
52 219 Amersham Biosciences (Amersham, England) and TrayCell (Hellma GmbH & Co. KG,
53
54 220 Müllheim, Germany))⁴³.
55
56
57
58
59
60

1
2
3 221
4
5
6 222 For the expression of HIS₆-TEV-GG-sfGFP, 50 ng plasmid DNA was used to transform *E. coli*
7
8 223 NiCo21(DE3) cells. Kanamycin containing, autoinducing ZYM-5052 growth media was
9
10 224 inoculated with an overnight culture³⁸. After 24 h incubation at 25°C the cells were harvested,
11
12 225 lysed and centrifuged as described above. The supernatant was applied on a HisTrap FF (GE
13
14 226 Healthcare Europe GmbH, Freiburg, Germany). After washing five times with wash buffer (25
15
16 227 mM TRIS-HCl pH 7.8, 300 mM NaCl, 20 mM Imidazole, Tween 20 0.25 % (v/v), 10 % (v/v)
17
18 228 glycerol) the bound protein was eluted (25 mM TRIS-HCl pH 7.8, 300 mM NaCl, 300 mM
19
20 229 Imidazole, Tween 20 0.25 % (v/v), 10 % (v/v) glycerol).
21
22
23
24

25 230
26
27 231 HIS₆-TEV-GG-sfGFP fusion protein (TEV cleavage site: ENLYFQG) was dialyzed immediately
28
29 232 after elution with the TEV protease (4°C, 50 mM TRIS-HCl, pH 7.0) overnight. The cleaved
30
31 233 product was separated from the uncleaved construct by applying the reaction mix on a HisTrap
32
33 234 FF 5 ml column. The successfully cut fragment in the flow through was collected. The fraction
34
35 235 was dialyzed against 50 mM TRIS-HCl, pH 7.0 and stored in 50 % (v/v) glycerol at -80°C. The
36
37 236 purity of the elution and the cleaved fraction was analyzed via a SDS-PAGE analysis. The
38
39 237 specific extinction coefficient of GFP at 485 nm was used to determine the concentration of GG-
40
41 238 sfGFP.
42
43
44
45

46 239
47
48 240 **Turbidity measurements.** For the turbidity measurements, a photometer with a Peltier heating
49
50 241 element was used (JASCO V-650, JASCO Germany GmbH, Gross-Umstadt, Germany). The
51
52 242 turbidity was determined at 350 nm while the temperature was ramped at a rate of 2°C/min.
53
54 243 Measurements were taken every 0.5°C between 20 and 80°C. ELPs were dialyzed against double
55
56
57
58
59
60

1
2
3 244 distilled water, mixed with a buffer stock solution (1 M TRIS-HCl, pH 7.0), sodium chloride
4
5 245 stock solution (3 M or 5 M) and adjusted with water to the desired final concentration.
6
7

8 246
9
10 247 For NaCl titration, 100 μ M of the ELP constructs were tested in a range of 0 - 3 M sodium
11
12 248 chloride. The 6x ELP construct was also probed in a concentration range of 25 μ M - 200 μ M
13
14 249 with different NaCl concentrations.
15

16 250
17
18 251 For pH titrations, stock solutions of 0.1 M phosphate-citrate buffer at different pH values were
19
20 252 mixed with solutions of water solubilized ELPs. Hereby a final concentration of 0.05 M of the
21
22 253 phosphate-citrate buffer was obtained.
23
24

25 254
26
27 255 Data analysis of the transition temperature curves (for NaCl, pH, concentration dependency and
28
29 256 PEG-ELP fusions) was performed by fitting the measured data points with a four-parameter
30
31 257 logistic function to obtain the corresponding transition temperature.
32
33

34 258
35
36 259 **Sortase and Sfp-mediated protein ligation.** For highest ligation efficiencies, enhanced Sortase
37
38 260 (eSortase) was used in the reaction⁴⁴. The reaction conditions for both Sfp and eSortase enzymes
39
40 261 were chosen according their reported reaction maxima to achieve highest activities²⁸. ELPs in
41
42 262 excess were added to a solution containing 50 mM TRIS-HCl, pH 7.5, 15 μ M ELP, 0.5 μ M GG-
43
44 263 sfGFP, 0.2 μ M eSortase, 1 μ M Sfp, 5 mM CaCl₂, 5 mM MgCl₂, 5 μ M CoA-647. The ligation
45
46 264 reaction was incubated for 2 h at 37°C.
47
48

49 265
50
51
52
53
54
55
56
57
58
59
60

1
2
3 266 **Cysteine-Maleimide bioconjugation reaction.** Cysteine-containing ELPs were reduced with 5
4
5
6 267 mM *tris(2-carboxyethyl)phosphine* (TCEP, (Thermo Fisher Scientific Inc., Waltham, MA,
7
8 268 USA)). After the removal of TCEP with ZebaTM Spin Desalting Columns 7K (Thermo Fisher
9
10 269 Scientific Inc., Waltham, MA, USA) cysteine-ELPs were mixed with Alexa₆₄₇-C2-Maleimide
11
12 270 (Thermo Fisher Scientific Inc., Waltham, MA, USA) and incubated for 1 h at 37°C (100 mM
13
14 271 TRIS-HCl, pH 7.0) (Supporting Information, Fig. S20).
15
16
17 272 PEG (MW: 20,000 Da, α -Methoxy- ω -maleimide, Rapp Polymere GmbH, Tübingen, Germany)
18
19 273 was used in different molar ratios in the bioconjugation reaction with cysteine-ELP₆₀ or ELP₆₀.
20
21
22 274 75 μ M of the reduced ELPs were mixed with TRIS-HCl (pH 7.0, 100 mM), PEG, and incubated
23
24 275 for 1 h at room temperature. After that they were mixed with 5 M NaCl and to a final
25
26 276 concentration of 3 M NaCl and their cloud point was determined as described above.
27
28
29
30
31

32 278 RESULTS AND DISCUSSION

33
34 279 Our sequence independent Golden Gate-based method provides an easy way to create defined
35
36 280 repetitive DNA sequences²⁶. We designed and produced gene cassettes encoding repetitive
37
38 281 proteins several hundreds of amino acids in length. Fig. 1 outlines the principle of primer design
39
40 282 and the following logical and stepwise workflow. The sequence of the starting synthetic gene
41
42 283 was designed in such a way that the codon usage within the first and last 15 nucleotides was
43
44 284 unique within the otherwise repetitive 150 bp sequence. This was necessary to ensure specific
45
46 285 annealing of primers at the 5' and 3' end. Desired modifications were introduced by overhangs
47
48 286 of the primers at their 5' end (i.e. *BsaI* recognition site) or at their 3' region (codon shuffling of
49
50 287 nucleotides). It was then possible to create 150 bp ELP genes with different flanking regions
51
52
53
54
55
56
57
58
59
60

1
2
3 288 from the same template (Primers 1-3; Fig. 1 A) using PCR primers that annealed at the 5' and 3'
4
5 289 ends of the synthetic gene.
6
7

8 290
9
10 291 In the first amplification and linearization reaction of the plasmid, primers annealed at the
11
12 292 desired ELP gene insertion site, i.e. at the opening location on the plasmid during the first PCR.
13
14 293 In our case this was downstream of the T7 promoter and upstream of the T7 terminator (see
15
16 294 Supporting Information Fig. S8 and S9). However, due to the freedom of primer design and
17
18 295 plasmid choice, the insertion site can in principle be anywhere in the plasmid. The primers
19
20 296 linearized the plasmid and introduced tags at the 5' (ybbR-tag) and 3' (Sortase c-tag) prime ends,
21
22 297 as well as *BsaI* recognition sites (Primers 5, 6; Vector A; Fig. 1 A). In our case, a modified
23
24 298 pET28a vector, already containing a ybbR-site downstream of the T7 promoter immediately
25
26 299 following the start codon AUG, served as template. Hence, only the Sortase c-tag was newly
27
28 300 introduced (see Supporting Information for primers for the standard pET28a vector). The
29
30 301 continuing general ELP expansion principle relies on having three different PCR amplified ELP
31
32 302 fragments (I, II, III) with different codon usages at their 5' and 3' end, within the *BsaI*-restriction
33
34 303 site (Supporting Information Fig. S1-S6). This design made logical and block-wise gene
35
36 304 assembly possible. The selected primers introduced a shuffled 3' end which matched the 5' end
37
38 305 of the subsequent fragment. In the first ELP assembly round, the 5' end of fragment I matched
39
40 306 the ybbR-tag of the linearized backbone. The 3' end of fragment III had compatible sticky ends
41
42 307 with the Sortase c-tag of the linearized plasmid (Fig. 1 B, 1st round). After successful annealing
43
44 308 of sticky ends, the T7 ligase covalently linked the three ELP fragments seamlessly into the
45
46 309 plasmid without any undesirable cloning scars in between.
47
48
49
50
51
52
53
54
55
56
57
58
59
60

1
2
3 311 The forward primer (Fig. 1 A, 2nd: Primer 7) for the following plasmid linearization rounds
4
5 312 annealed at a different site within the ELP-containing plasmid, compared to the initial
6
7
8 313 linearization round (Fig. 1 A, 1st: Primer 5). It annealed at the ybbR-tag and the 5' end of the
9
10 314 ELP gene. Right in between the two coding regions, a non-annealing loop encoding a *BsaI*
11
12 315 recognition site was introduced (Fig. 1 A 2nd, and Fig. 1 B 2nd round) with the primer. The
13
14
15 316 annealing at the ybbR-tag was necessary to ensure high temperature-dependent primer annealing
16
17 317 specificity at the very 5' end of the ELP gene, otherwise the primer would anneal at every
18
19
20 318 fragment I throughout the whole assembled ELP gene cassette. High annealing temperatures
21
22 319 minimize undesired PCR side products, i.e. only partly ELP-containing, linearized vectors. The
23
24 320 reverse primer was the same for all plasmid linearization reactions (Fig. 1 A; Vector B). After
25
26
27 321 the restriction digestion reaction, the linear plasmid now had a Sortase c-tag sticky end at the 3'
28
29 322 end and an ELP fragment I sticky end at the 5' end.
30
31

32 323
33
34 324 Now only the last ELP fragment (Fig. 1 A, Insert IV) had to be amplified with a different reverse
35
36 325 primer (Fig. 1 A, Primer 4) to yield a PCR product with a compatible 3' end to the already
37
38 326 existing ELP cassette. The growing ELP insert in the plasmid always started with fragment I.
39
40 327 This made the reuse of the amplified insert sequences (I, II, IV) for every following expansion
41
42 328 cloning round possible (Fig. 1 B, >3rd rounds).
43
44
45
46 329

47
48 330 This method not only allows a logical assembly of repetitive gene patterns, but also makes the
49
50 331 modification of flanking regions or mutation of the first base pairs at 5' end 3' end possible. For
51
52 332 example, we introduced two glutamates in each of the fragments at their 5' and 3' ends by
53
54 333 changing the codon from the 'X' guest residue at the 5' and 3' end of the VPGXG motif to a
55
56
57
58
59
60

1
2
3 334 glutamate (VPGEG). The primers did not align completely with the template and introduced the
4
5 335 glutamate mutation during PCR amplification. The chemically synthesized sequence also had
6
7
8 336 some minor mistakes at the 3' end, which were corrected with primers within the initial PCR.
9
10 337 The final ELP substructure of all ELPs used in this study consisted of 10 pentapeptide repeats
11
12 338 (VPGXG₁₀, X being [EV₄A₂G₂E]). For the rest of the manuscript this motif is referred as ELP_n
13
14
15 339 with n being the number of pentapeptide repeats of this motif (see Supporting Information, DNA
16
17 340 Sequence 2, Protein Sequence 2 and DNA Sequence 7, Protein Sequence 3).
18
19

20 341
21
22 342 We ligated three 150 bp fragments with a linearized vector of choice in one step. It was possible
23
24 343 to modify the 5' and 3' ends of the fragments with overhang primers prior to ligation, in our case
25
26 344 with an N-terminal ybbR and a C-terminal Sortase tag (Fig. 1 B). Overall seven different ELP
27
28 345 constructs were used in this study for biophysical characterization of the peptide sequence, while
29
30 346 ten were successfully cloned. The largest ELP gene contained 120 pentapeptide repeats. All ELP
31
32 347 constructs were built with the four different ELP PCR products from the same batch. PCR gels
33
34 348 from the fragments and an overview of cloning efficiencies can be found in the supporting
35
36 349 information (Fig. S9 and Tab. S1). Typical yields after the purification were 56 – 138 mg
37
38 350 Protein/l culture, while the ELP₁₀ repeat had the lowest yield (2 mg Protein/l culture).
39
40
41
42
43
44

45
46 351
47 352 Tab. 2 shows biophysical characteristics of the ELPs characterized in this study. Each ELP was
48
49 353 produced with a ybbR-tag at the N-terminus and a Sortase c-tag at the C-terminus. In the bottom
50
51 354 right corner of the schematic (Fig. 1), FD-*Eco*RI digested plasmids are shown on an agarose gel.
52
53 355 The gel analysis shows the successful construction of plasmids containing 10 to 120
54
55 356 pentapeptide repeats.
56
57
58
59
60

357 **Table 2.** Biophysical properties of the characterized ELP constructs.

ELP repeats (5) _x	ϵ_{205} [1/M cm] ⁴³	Molecular weight [Da] ⁴⁵	Glutamate residues in ELP repeat	Isoelectric point ⁴⁵	Amino acids in ELP repeats (total)	Total Length [nm] ⁴⁶
10	196690	5893.7	2	3.91	50 (68)	24.82
20	335690	9908.2	4	3.77	100 (118)	43.07
30	474690	13922.8	6	3.67	150 (168)	61.32
40	613690	17937.3	8	3.59	200 (218)	79.57
50	752690	21951.9	10	3.53	250 (268)	97.82
60	891960	25966.4	12	3.47	300 (318)	116.07
Cys-60	855980	24894.2	12	3.20	300 (308)	112.42

358

359 Following successful cloning, expression and purification, we tested the functionality of the

360 attached terminal tags. Fig. 2 A shows the scheme for post-translational protein ligation

361 reactions. The ELPs of varying lengths contain an N-terminal ybbR-tag and a C-terminal Sortase

362 recognition sequence (i.e., LPETGG). Subpanel 2 B to 2 C show an SDS-PAGE image of the

363 same gel with different excitation and emission filters. Using a reaction catalyzed by Sfp, it was

364 possible to fuse a fluorescently labeled CoA-647 to the ELP (N-terminal ybbR-tag). Results of

365 the specific excitation for the CoA-647 dye are shown in 2 B. Brightest are the CoA-647-ELP

366 fusions proteins, but also the CoA-647-ELP-sfGFP fusion proteins are visible above the bright

367 monomer band. Fully denatured proteins appear slightly higher in the gel due to their different

1
2
3 368 running behavior. The Sortase-tag was simultaneously utilized for fusion of different proteins to
4
5 369 the ELP sequences (C-terminal LPETGG). A GG-sfGFP was fused to the ELPs, which was
6
7
8 370 excited with blue LED light and detected within the green emission of sfGFP (Fig. 2 C). Non-
9
10 371 ligated and non-denaturated GFP appears at the top of the gel, since it does not run according its
11
12 372 molecular weight in its native (i.e., correctly folded) state (see Supporting Information, Fig.
13
14 373 S12). No GFP fluorescence is visible in the heated samples due to complete denaturation of the
15
16 374 GFP chromophore. Panel 2 D shows an overlay of B and C, visualizing the successful post-
17
18 375 translational ligation of GG-sfGFP and CoA-647 to the different ELP peptides within a one-pot
19
20 376 reaction. The ligation efficiency of the Sortase never goes to 100 % completion. Due to the
21
22 377 Sortase reaction mechanism, a dynamic equilibrium is eventually reached and complete fusion of
23
24 378 GG-sfGFP to ELP is therefore not to be expected⁴⁷.

25
26 379
27
28 380 After confirming the biochemical accessibility and functionality of the terminal ybbR- and
29
30 381 Sortase-tags, we characterized the phase behavior of the modified ELPs. Fig. 3 presents an
31
32 382 overview of the lower critical solution temperatures (LCSTs) of the characterized ELPs under
33
34 383 various conditions. First the temperature dependence of the ELP₁₀₋₆₀ constructs were probed
35
36 384 against different sodium chloride concentrations, at neutral pH (50 mM TRIS-HCl, pH 7.0) (Fig.
37
38 385 3 A). The 10 pentapeptide repeat ELP did not collapse below 80°C, which is in agreement with
39
40 386 the remainder of the data set if one looks at the increasing transition temperature with decreasing
41
42 387 size of the construct. The 20 pentapeptide ELP repeat, for example, only collapsed with 3 M of
43
44 388 sodium chloride at 60°C. Fig. 3 B clarifies the correlation between salt concentration, molecular
45
46 389 mass and transition temperatures. Only the longest ELP construct collapsed across all given
47
48 390 sodium chloride concentrations in the temperature range from 20 to 80°C. Salt-induced cloud
49
50 391 point shifts are a well known characteristic of ELPs^{15,24,48}.

1
2
3 392
4
5 393 The incorporation of two glutamates per ten pentapeptides resulted in pH-dependent transitions.
6
7
8 394 ELPs with glutamates were expected to show pH-responsiveness. Above their pK_a the ELPs have
9
10 395 a relatively high transition temperature, since the glutamates are deprotonated and ionized and
11
12 396 therefore electrostatically repel each other. Below or close to their corresponding pK_a , the
13
14
15 397 transition temperature significantly decreases due to protonation and neutralization of the
16
17 398 negative charge (Fig. 3 C). The decreasing influence of salt at lower pH is similar to that
18
19 399 demonstrated by MacKay *et al.*⁴⁹. Fig. 3 D illustrates the dependence of transition temperature
20
21 400 on the ELP concentration. At concentrations above 100 μ M, the 60 pentapeptide ELP (150, 200
22
23 401 μ M) already collapsed at room temperature, hence it was not possible to determine an exact
24
25
26 402 transition point. The ligated product between the 60 pentapeptide ELP repeat and the sfGFP did
27
28 403 not show any transition compared to the pure 60 pentapeptide ELP (data not shown). This
29
30
31 404 concentration dependence is also a well-known characteristic of ELPs¹⁰.

32
33
34 405
35
36 406 This PCR based method can also be employed to change the flanking sequences of the ELP very
37
38 407 quickly. Fig. 4 A shows the underlining principle of the cloning procedure used to install
39
40 408 cysteine as an end residue with no cloning scar. Due to the repetitive structure of the ELP gene it
41
42
43 409 was necessary to design primers which anneal at the site of replacement. A *BsaI* recognition loop
44
45
46 410 between ELP annealing and deletion annealing site was necessary to remove the deletion site
47
48 411 again afterwards. *BsaI* digestion left incompatible 5' and 3' sticky ends, therefore a Klenow
49
50 412 Fragment was employed to fill the ends. A standard blunt end ligation circularized the linear
51
52
53 413 plasmid (Fig. 4A and Supporting Information: Fig. S13-S18). This procedure provided an N-
54
55 414 terminal cysteine that could be used for bioconjugations to various (macro)molecules (see
56
57 415 Supporting Information, DNA Sequence 9, Protein Sequence 5). The cysteine in the ELP is able
58
59
60

1
2
3 416 to form disulfide bonds with different cysteine containing proteins, but also is able to be clicked
4
5
6 417 to other reactive groups like maleimide (i.e. a maleimide-PEG (Fig. 4 B)). The cloud point
7
8 418 determination of Fig. 4 C shows the influence of PEG conjugation on the ELP cloud point,
9
10 419 confirming a shift towards higher temperatures (Fig. 4 C, CYS-ELP₆₀) due to conjugation of the
11
12 420 hydrophilic synthetic polymer. However, the same PEG added to a solution of the same ELP that
13
14 421 lacked the cysteine functionality did not significantly influence the cloud point (Fig. 4 C, ELP₆₀).
15
16
17
18 422
19
20

21 423 CONCLUSION

22
23 424 The presented approach shows an alternative way to create fast and convenient functional ELPs
24
25 425 with sequence lengths up to 600 amino acids, or hundreds of nm in stretched contour length. It
26
27
28 426 allows a straightforward fusion of gene sequences encoding the ELP repeats without any prior
29
30 427 vector modifications. We used this approach to demonstrate facile incorporation of functional
31
32 428 peptide tags as end groups into ELPs. We demonstrate how this approach was useful for
33
34 429 developing end-labeled ELPs through enzyme-mediated site-specific ligation to organic dyes and
35
36
37 430 fluorescent proteins, and show how terminal cysteine incorporation expands the versatile toolbox
38
39
40 431 of bioconjugation opportunities. Since we used a PCR and primer-based approach, our method is
41
42 432 essentially sequence independent and does not leave cloning scars. In the future we anticipate
43
44 433 that such a tool for straightforward end-group modification of ELPs will prove useful for
45
46
47 434 developing custom engineered macromolecular systems.
48

49 435

50 51 436 ASSOCIATED CONTENT

52 53 54 55 437 **Supporting Information**

1
2
3 438 Additional information including sequence data (DNA and Protein sequences), extended cloning
4
5 439 procedures and gel pictures of PCR products and protein purification steps.
6
7

8
9 440 This material is available free of charge via the Internet at <http://pubs.acs.org>.
10

11 441

12 442 **AUTHOR INFORMATION**

13 443 **Corresponding Author**

14
15
16 444 e-Mail: *michael.nash@lmu.de
17
18

19 445 **Author Contributions**

20 446 W.O., M.A.N. and H.E.G. designed the research; W.O. and T. N. performed experiments; W.O.
21
22 447 performed data analysis; W.O., and M.A.N. co-wrote the manuscript.
23
24

25 448 **Notes**

26 449 The authors declare no competing financial interests.
27
28 450

29 451 **ACKNOWLEDGMENT**

30
31
32
33
34 452 We gratefully acknowledge funding from an advanced grant of the European Research Council
35 453 (Cellufuel Grant 294438), SFB 863 and the Excellence Cluster Center for Integrated Protein
36 454 Science Munich. M.A.N. acknowledges funding from Society in Science - The Branco Weiss
37 455 Fellowship program administered by ETH Zürich, Switzerland. We thank the systems biophysics
38 456 group of Professor Dieter Braun (Ludwig-Maximilians-Universität München) for the access to
39 457 the JASCO V-650. The authors thank Anna Krautloher for initial concentration determinations
40 458 of the ELPs at 205 nm. We acknowledge Markus Jobst for his advice on the ongoing manuscript.
41
42 459 We thank the following people for providing material to this study: Ellis Durner (eSortase),
43
44
45
46
47
48
49
50
51
52
53
54
55
56
57
58
59
60

1
2
3 460 Angelika Kardinal (TEV protease) and Diana Pippig (Sfp), and Arne Goldenbaum for assistance
4
5
6 461 in lab work. We are grateful for the MALDI-TOF analysis of ELP samples by the protein
7
8 462 analysis group of the Ludwig-Maximilians-Universität München (Professor Axel Imhof, Dr.
9
10 463 Andreas Schmidt, Dr. Ignasi Forné and Pierre Schilcher).
11
12

13
14 464 REFERENCES

- 15 465 (1) Pack, D. W.; Hoffman, A. S.; Pun, S.; Stayton, P. S. *Nat. Rev. Drug Discov.* **2005**, *4* (7),
16 466 581–593.
- 17
18 467 (2) Onaca, O.; Enea, R.; Hughes, D. W.; Meier, W. *Macromol. Biosci.* **2009**, *9* (2), 129–139.
- 19
20 468 (3) Nash, M. A.; Waitumbi, J. N.; Hoffman, A. S.; Yager, P.; Stayton, P. S. *ACS Nano* **2012**,
21 469 *6* (8), 6776–6785.
- 22
23 470 (4) Nash, M. A.; Gaub, H. E. *ACS Nano* **2012**, *6* (12), 10735–10742.
- 24
25 471 (5) Urry, D. W.; Hugel, T.; Seitz, M.; Gaub, H. E.; Sheiba, L.; Dea, J.; Xu, J.; Parker, T.
26 472 *Philos. Trans. R. Soc. B Biol. Sci.* **2002**, *357* (1418), 169–184.
- 27
28 473 (6) Wolff, M.; Braun, D.; Nash, M. A. *Anal. Chem.* **2014**, *86* (14), 6797–6803.
- 29
30 474 (7) Urry, D. W.; Haynes, B.; Harris, R. D. *Biochem. Biophys. Res. Commun.* **1986**, *141* (2),
31 475 749–755.
- 32
33 476 (8) Tatham, A. S.; Shewry, P. R. *Trends Biochem. Sci.* **2000**, *25* (11), 567–571.
- 34
35 477 (9) Urry, D. W.; Haynes, B.; Zhang, H.; Harris, R. D.; Prasad, K. U. *Proc. Natl. Acad. Sci. U.*
36 478 *S. A.* **1988**, *85* (10), 3407–3411.
- 37
38 479 (10) Meyer, D. E.; Chilkoti, A. *Biomacromolecules* **2004**, *5* (3), 846–851.
- 39
40 480 (11) Urry, D. W. *J. Phys. Chem. B* **1997**, *101* (51), 11007–11028.
- 41
42 481 (12) Bataille, L.; Dieryck, W.; Hocquellet, A.; Cabanne, C.; Bathany, K. *PROTEIN Expr.*
43 482 *Purif.* **2015**, *110*, 165–171.
- 44
45 483 (13) Bellucci, J. J.; Amiram, M.; Bhattacharyya, J.; McCafferty, D.; Chilkoti, A. *Angew.*
46 484 *Chemie - Int. Ed.* **2013**, *52* (13), 3703–3708.
- 47
48 485 (14) Meyer, D. E.; Chilkoti, A. *Nat. Biotechnol.* **1999**, *17* (11), 1112–1115.
- 49
50 486 (15) Gagner, J. E.; Kim, W.; Chaikof, E. L. *Acta Biomater.* **2014**, *10* (4), 1542–1557.
- 51
52 487 (16) Kojima, C.; Irie, K. *Biopolymers* **2013**, *100* (6), 714–721.
- 53
54 488 (17) Christensen, T.; Hassouneh, W.; Trabbic-Carlson, K.; Chilkoti, A. *Biomacromolecules*
- 55
56
57
58
59
60

- 1
2
3 489 2013, 14 (5), 1514–1519.
4
5 490 (18) McDaniel, J. R.; Radford, D. C.; Chilkoti, A. *Biomacromolecules* 2013, 14 (8), 2866–
6 491 2872.
7
8 492 (19) Rousseau, R.; Schreiner, E.; Kohlmeyer, A.; Marx, D. *Biophys. J.* 2004, 86 (3), 1393–
9 493 1407.
10
11 494 (20) Qin, G.; Glassman, M. J.; Lam, C. N.; Chang, D.; Schaible, E.; Hexemer, A.; Olsen, B. D.
12 495 *Adv. Funct. Mater.* 2014, 25 (5), 729–738.
13
14 496 (21) Glaves, R.; Baer, M.; Schreiner, E.; Stoll, R.; Marx, D. *ChemPhysChem* 2008, 9 (18),
15 497 2759–2765.
16
17 498 (22) Wang, H.; Cai, L.; Paul, A.; Enejder, A.; Heilshorn, S. C. *Biomacromolecules* 2014, 15
18 499 (9), 3421–3428.
19
20 500 (23) Van Eldijk, M. B.; Smits, F. C. M.; Vermue, N.; Debets, M. F.; Schoffelen, S.; Van Hest,
21 501 J. C. M. *Biomacromolecules* 2014, 15 (7), 2751–2759.
22
23 502 (24) Meyer, D. E.; Chilkoti, A. *Biomacromolecules* 2002, 3 (2), 357–367.
24
25 503 (25) Amiram, M.; Quiroz, F. G.; Callahan, D. J.; Chilkoti, A. *Nat. Mater.* 2011, 10 (2), 141–
26 504 148.
27
28 505 (26) Engler, C.; Kandzia, R.; Marillonnet, S. *PLoS One* 2008, 3 (11), e3647.
29
30 506 (27) McDaniel, J. R.; MacKay, J. A.; Quiroz, F. G.; Chilkoti, A. *Biomacromolecules* 2010, 11
31 507 (4), 944–952.
32
33 508 (28) Yin, J.; Lin, A. J.; Golan, D. E.; Walsh, C. T. *Nat. Protoc.* 2006, 1 (1), 280–285.
34
35 509 (29) Huber, M. C.; Schreiber, A.; Wild, W.; Benz, K.; Schiller, S. M. *Biomaterials* 2014, 35
36 510 (31), 8767–8779.
37
38 511 (30) Christensen, T.; Amiram, M.; Dagher, S.; Trabbic-Carlson, K.; Shamji, M. F.; Setton, L.
39 512 A.; Chilkoti, A. *Protein Sci.* 2009, 18 (7), 1377–1387.
40
41 513 (31) Beerli, R. R.; Hell, T.; Merkel, A. S.; Grawunder, U. *PLoS One* 2015, 10 (7), e0131177.
42
43 514 (32) Qi, Y.; Amiram, M.; Gao, W.; McCafferty, D. G.; Chilkoti, A. *Macromol. Rapid*
44 515 *Commun.* 2013, 34, 1256–1260.
45
46 516 (33) Mazmanian, S. K.; Liu, G.; Ton-That, H.; Schneewind, O. *Science* 1999, 285 (5428), 760–
47 517 763.
48
49 518 (34) Yin, J.; Straight, P. D.; McLoughlin, S. M.; Zhou, Z.; Lin, A. J.; Golan, D. E.; Kelleher,
50 519 N. L.; Kolter, R.; Walsh, C. T. *Proc. Natl. Acad. Sci. U. S. A.* 2005, 102 (44), 15815–
51 520 15820.
52
53 521 (35) Gibson, D. G.; Young, L.; Chuang, R.-Y.; Venter, C. J.; Hutchison III, C. A.; Smith, H. O.
54
55
56
57
58
59
60

- 1
2
3 522 *Nat. Methods* **2009**, *6* (5), 343–347.
- 4
5 523 (36) Otten, M.; Ott, W.; Jobst, M. A.; Milles, L. F.; Verdorfer, T.; Pippig, D. A.; Nash, M. A.;
6 524 Gaub, H. E. *Nat. Methods* **2014**, *11* (11), 1127–1130.
- 7
8 525 (37) Robichon, C.; Luo, J.; Causey, T. B.; Benner, J. S.; Samuelson, J. C. *Appl. Environ.*
9 526 *Microbiol.* **2011**, *77* (13), 4634–4646.
- 10 527 (38) Studier, F. W. *Protein Expr. Purif.* **2005**, *41*, 207–234.
- 11
12 528 (39) Collins, T.; Azevedo-Silva, J.; da Costa, A.; Branca, F.; Machado, R.; Casal, M. *Microb.*
13 529 *Cell Fact.* **2013**, *12* (21), 1–16.
- 14
15 530 (40) Chow, D. C.; Dreher, M. R.; Trabbic-Carlson, K.; Chilkoti, A. *Biotechnol. Prog.* **2006**, *22*
16 531 (3), 638–646.
- 17
18 532 (41) MacEwan, S. R.; Hassouneh, W.; Chilkoti, A. *J. Vis. Exp.* **2014**, No. 88, e51583.
- 19
20 533 (42) Laemmli, U. K. *Nature* **1970**, *227* (5259), 680–685.
- 21
22 534 (43) Anthis, N. J.; Clore, G. M. *Protein Sci.* **2013**, *22* (6), 851–858.
- 23
24 535 (44) Dorr, B. M.; Ham, H. O.; An, C.; Chaikof, E. L.; Liu, D. R. *Proc. Natl. Acad. Sci.* **2014**,
25 536 *111* (37), 13343–13348.
- 26
27 537 (45) Gasteiger, E.; Hoogland, C.; Gattiker, A.; Duvaud, S.; Wilkins, M. R.; Appel, R. D.;
28 538 Bairoch, A. In *The Proteomics Protocols Handbook*; 2005; pp 571–607.
- 29
30 539 (46) Dietz, H.; Rief, M. *Proc. Natl. Acad. Sci. U. S. A.* **2006**, *103* (5), 1244–1247.
- 31
32 540 (47) Theile, C.; Witte, M.; Blom, A. *Nat. Protoc.* **2013**, *8* (9), 1800–1807.
- 33
34 541 (48) Catherine, C.; Oh, S. J.; Lee, K.-H.; Min, S.-E.; Won, J.-I.; Yun, H.; Kim, D.-M.
35 542 *Biotechnol. Bioprocess Eng.* **2015**, *20* (3), 417–422.
- 36
37 543 (49) MacKay, J. A.; Callahan, D. J.; FitzGerald, K. N.; Chilkoti, A. *Biomacromolecules* **2010**,
38 544 *11* (11), 2873–2879.
- 39
40
41
42
43 545
44
45
46
47
48
49
50
51
52
53
54
55
56
57
58
59
60

546 FIGURE CAPTIONS

547 **Figure 1.** Cloning schematic

548 (A) The schematic describes the process of sequence independent PCR amplification of unique
549 inserts (I, II, III) from the same template. The amplification of the first backbone (plasmid A)
550 enables subcloning of the first three inserts, which leads to plasmid B. Plasmid B is linearized at
551 the N-terminal ybbR-tag, as are all the following backbones. The new ELP amplicons can always
552 be inserted upstream of the old ELP repeats. (B) Repetitive rounds of cloning add subsequently
553 more ELP inserts until the desired length is achieved.

554 **Figure 2.** Post-translational ligation of the ELP peptide

555 (A) Schematic of the ELP constructs containing a N-terminal ybbR-tag and a C-terminal Sortase-
556 tag. A post-translational one-pot reaction was used to fuse a CoA-647 fluorescent dye to the N-
557 Termini via an Sfp-catalyzed reaction. In parallel, the eSortase fuses a GG-sfGFP towards the C-
558 terminal LPETGG. (B) An image of a SDS gel obtained following dual labeling of ELPs under
559 different reaction conditions and ELP lengths. The image shows only the red CoA-647 dye (ex:
560 530/28, em: 695/55 nm). (C) Fluorescent image of the same gel as in B, but this time with blue
561 excitation (ex: 470/530, em: 530/28 nm), hence only the native GFP specific bands are visible.
562 (D) Overlay of B and C plus additional UV illumination which excites tryptophan side group
563 converted fluorophores enabled by the Bio-Rad Stain-FreeTM technology.

564 **Figure 3.** Cloud point characterization of the 10 – 60 pentapeptide ELP repeats

565 (A) shows the characteristic decrease in the transition temperature of the ELPs with increasing
566 sodium chloride concentration and ELP length. (B) illustrates the relation between increasing
567 transition temperature and decreasing molecular weight. (C) shows the correlation between pH,
568 NaCl and transition temperature. (D) shows the concentration dependency of the transition
569 temperature for the 60 pentapeptide ELP repeat. Data points for the plots were obtained from
570 triplicates. Error bars represent the standard deviation of the average transition point.

571 **Figure 4.** Cloning schematic and bioconjugation of cysteine-ELPs with a maleimide-dye and
572 PEG-maleimide.

573 (A) Illustration of the cloning schematic for changing the ELP flanking regions (i.e. replacement
574 of the ybbR-sequence with a cysteine). The ybbR-sequence was deleted *via* a PCR reaction, and
575 a cysteine was introduced (see Primers 10 and 11 in Table 1). The flanking restriction sites were
576 digested with *BsaI*-HF and the remaining sticky ends were filled in with Klenow Fragment.
577 Finally, the linear product was circularized with T4 ligase. (B) Procedure of the bioconjugation
578 reaction. Cysteine-ELPs were reduced with TCEP and conjugated to a maleimide dye or a PEG-
579 maleimide polymer. A gel image on the right shows the successful conjugation reaction between
580 the dye and the ELP. (C) Bioconjugation of a 20 kDa PEG-maleimide to CYS-ELP₆₀ shifted the
581 cloud point up by ~4°C (left panel). The cloud point of ELP₆₀ lacking cysteine (middle panel)
582 was not influenced by the addition of maleimide PEG. The right panel shows the cloud point
583 shift (ΔT) due to addition of different concentrations of PEG-maleimide. Data points for the plot
584 were obtained from triplicates. Error bars account for Gaussian error propagation due to
585 calculation of the difference of the average transition point from three samples.

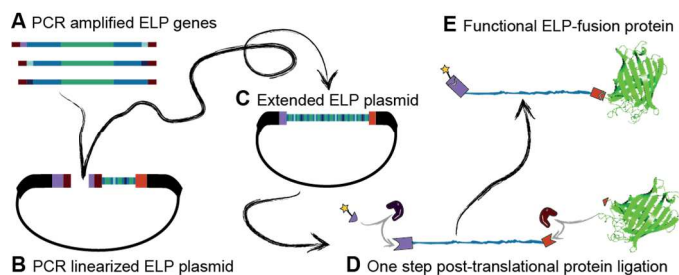
1
2
3 586 For Table of Contents Use Only
4

5
6 587 Sequence Independent Cloning and Post-translational Modification of Repetitive Protein
7

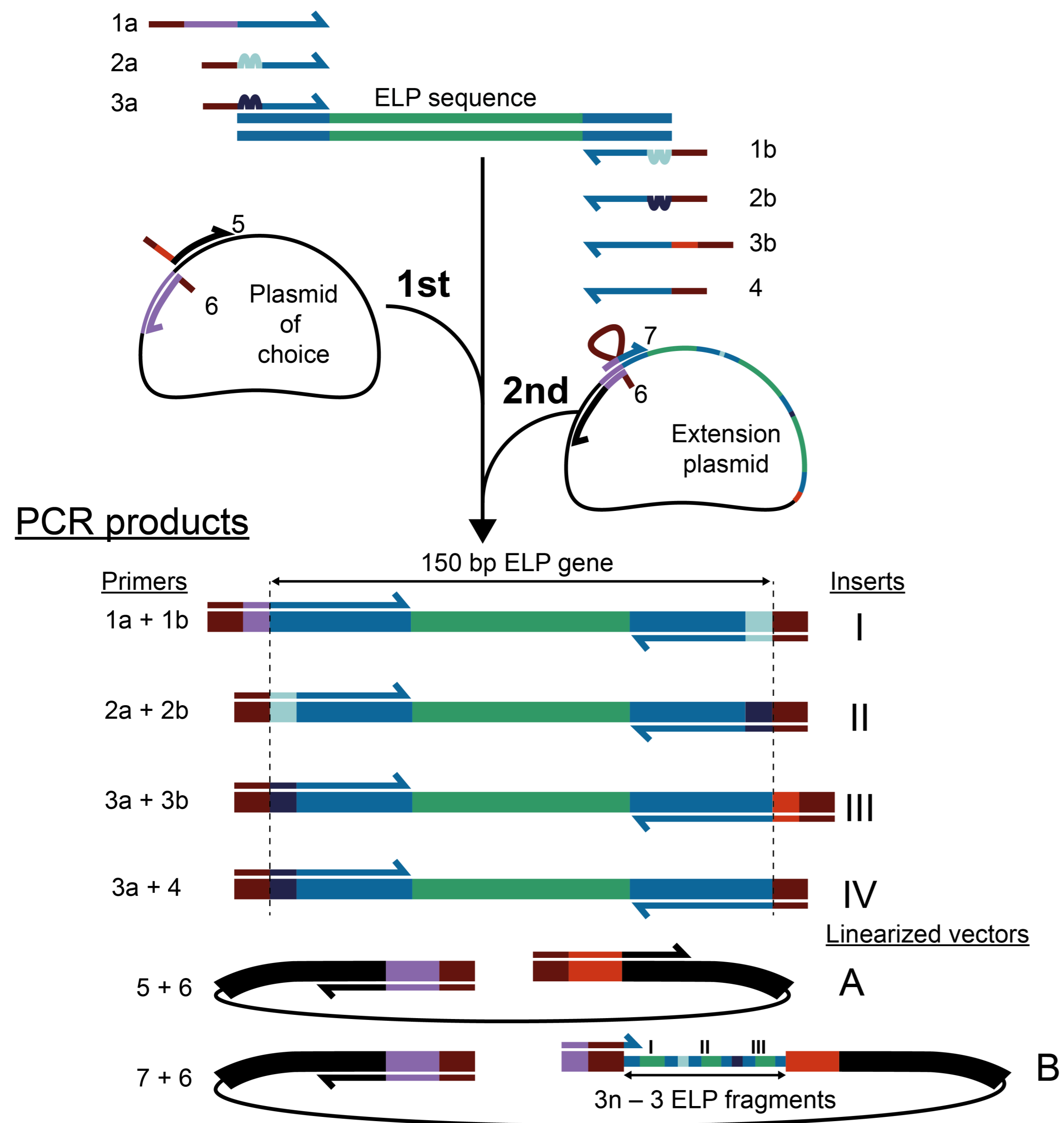
8 588 Polymers through Sortase and Sfp-mediated Enzymatic Ligation
9

10
11 589 Wolfgang Ott, Thomas Nicolaus, Hermann E. Gaub and Michael A. Nash
12
13

14
15
16
17
18
19
20
21
22
23
24 590

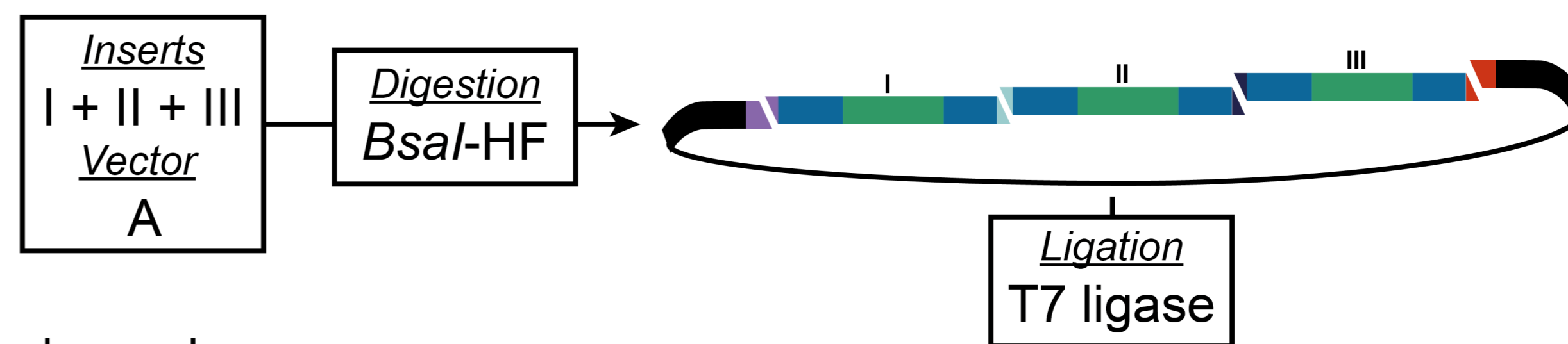


A Primers and starting material

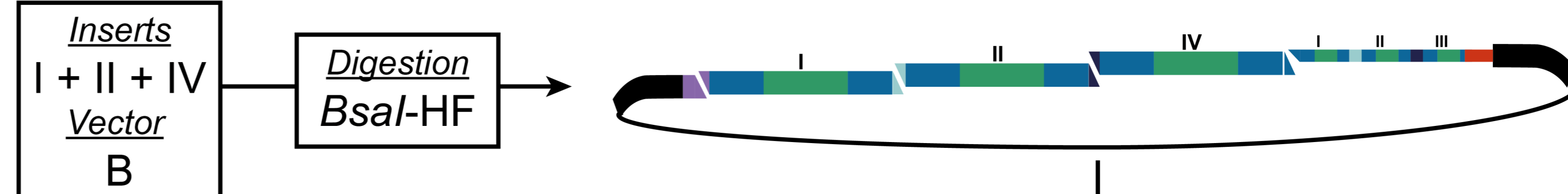


B Cloning procedure

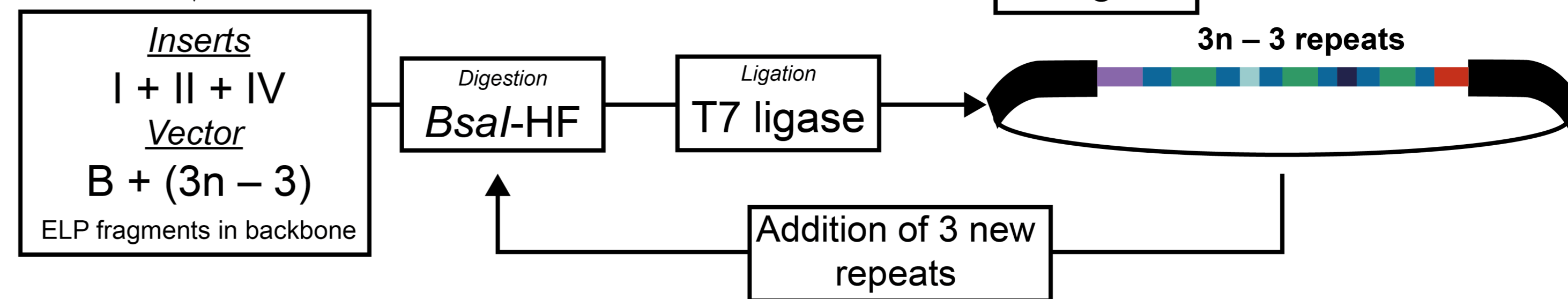
1st round



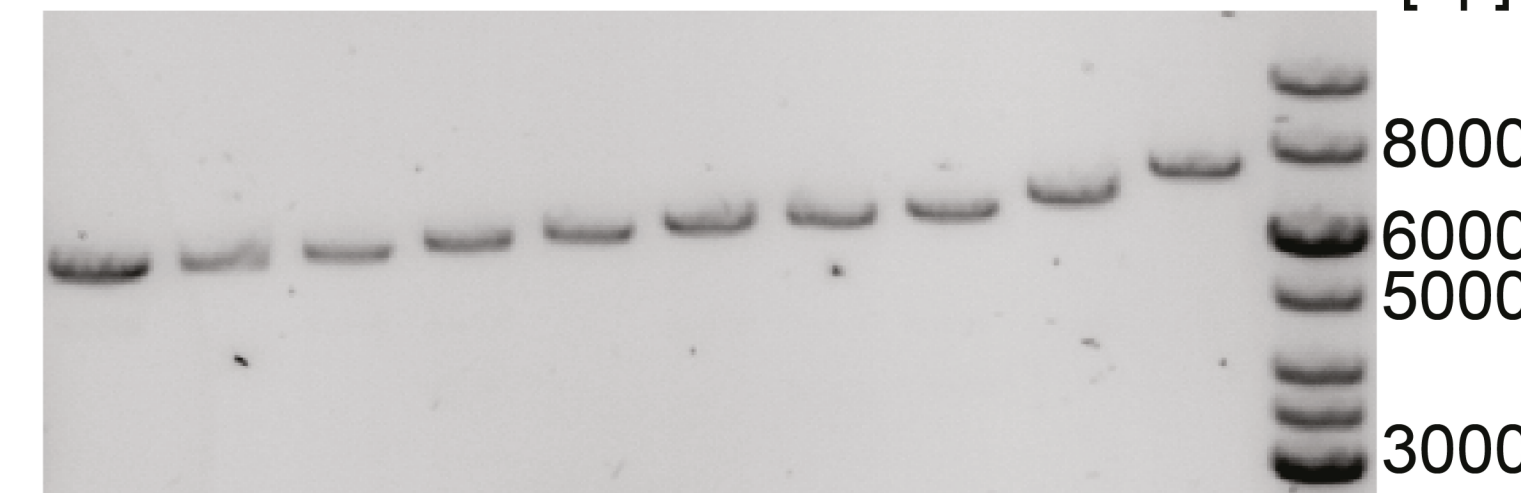
2nd round



>3rd rounds



1x 2x 3x 4x 5x 6x 7x 8x 9x 12x [bp]



ELP

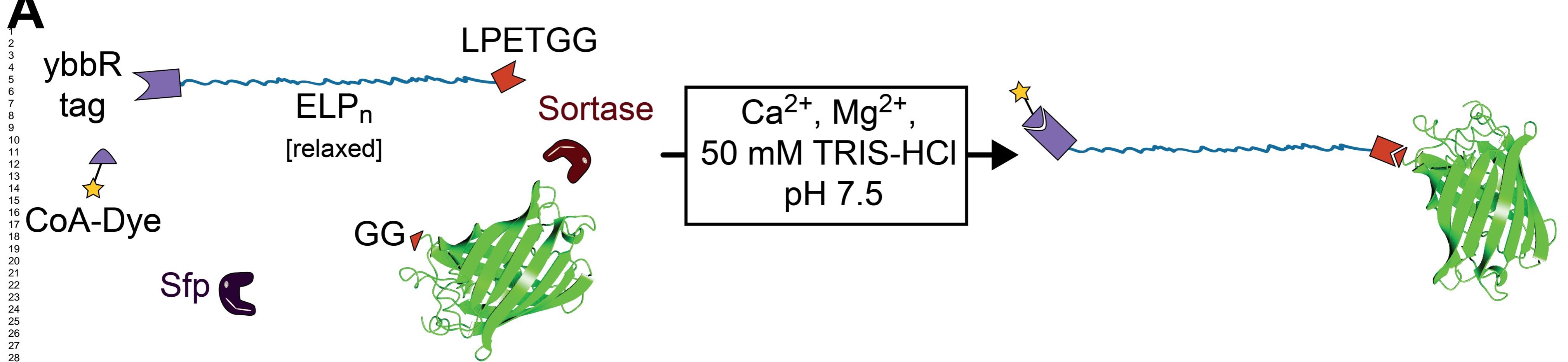
ELP (codon shuffled)

ybbR-tag

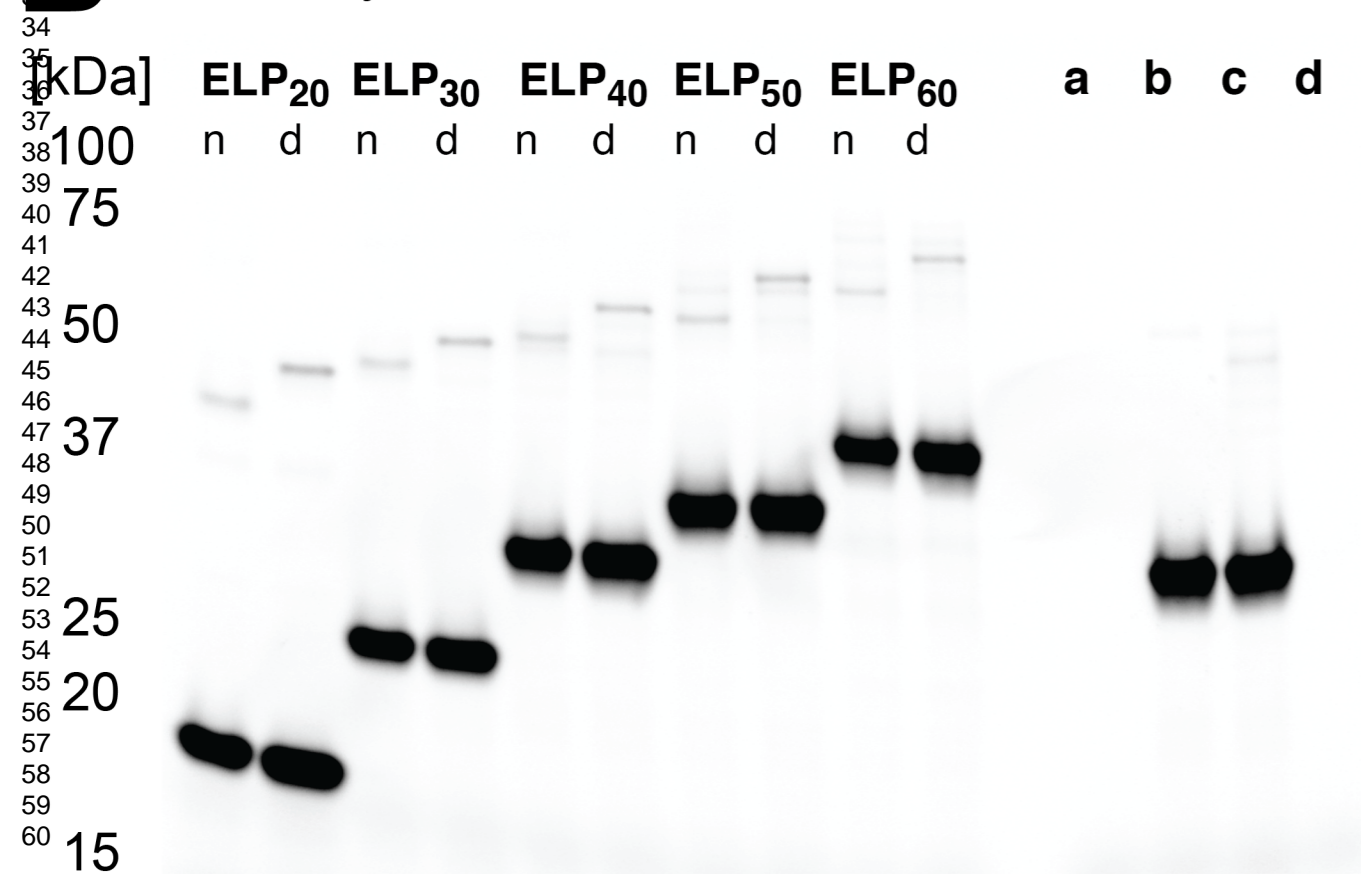
Sortase c-tag

BsaI restriction site

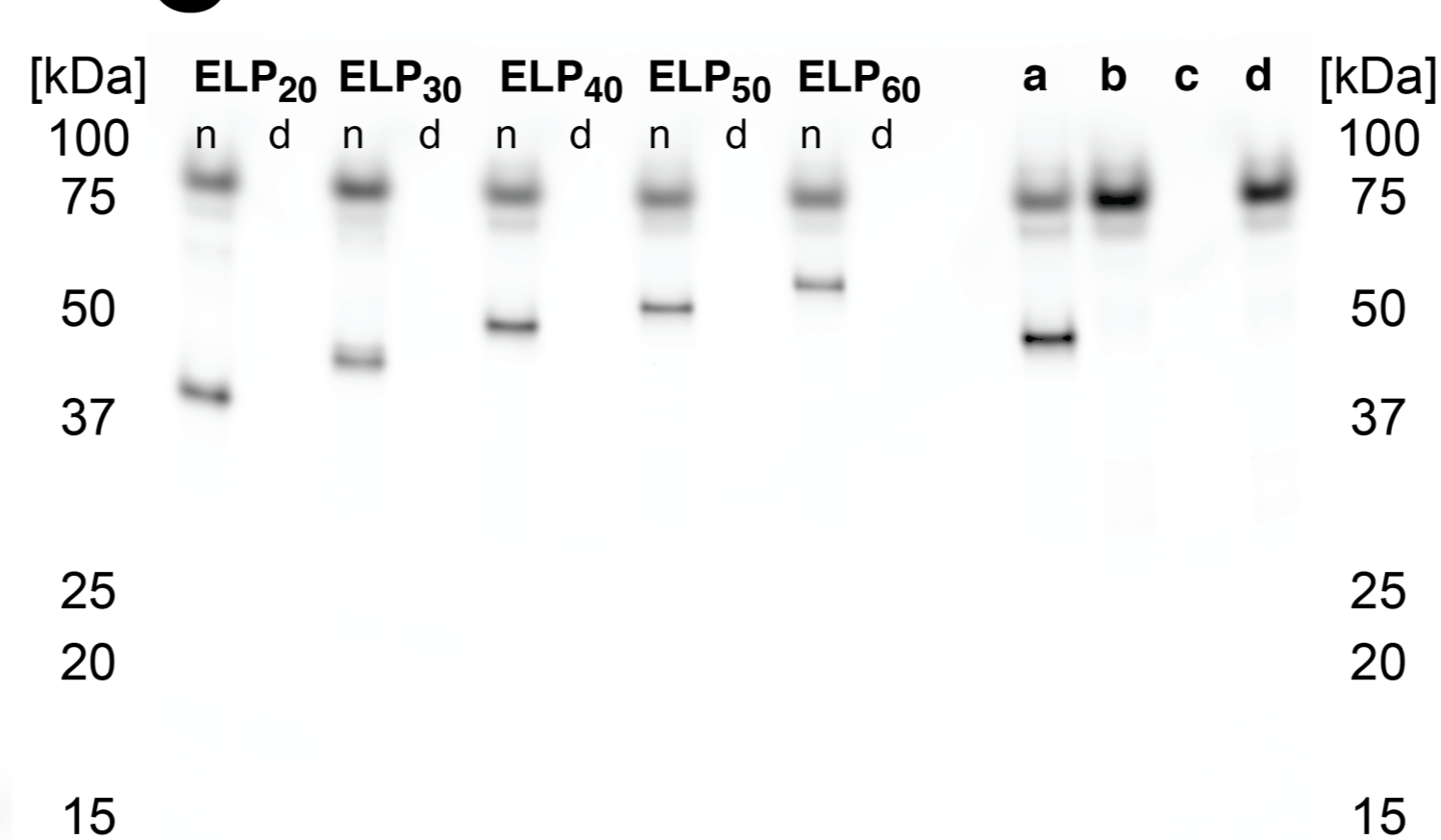
n: number of cloning rounds



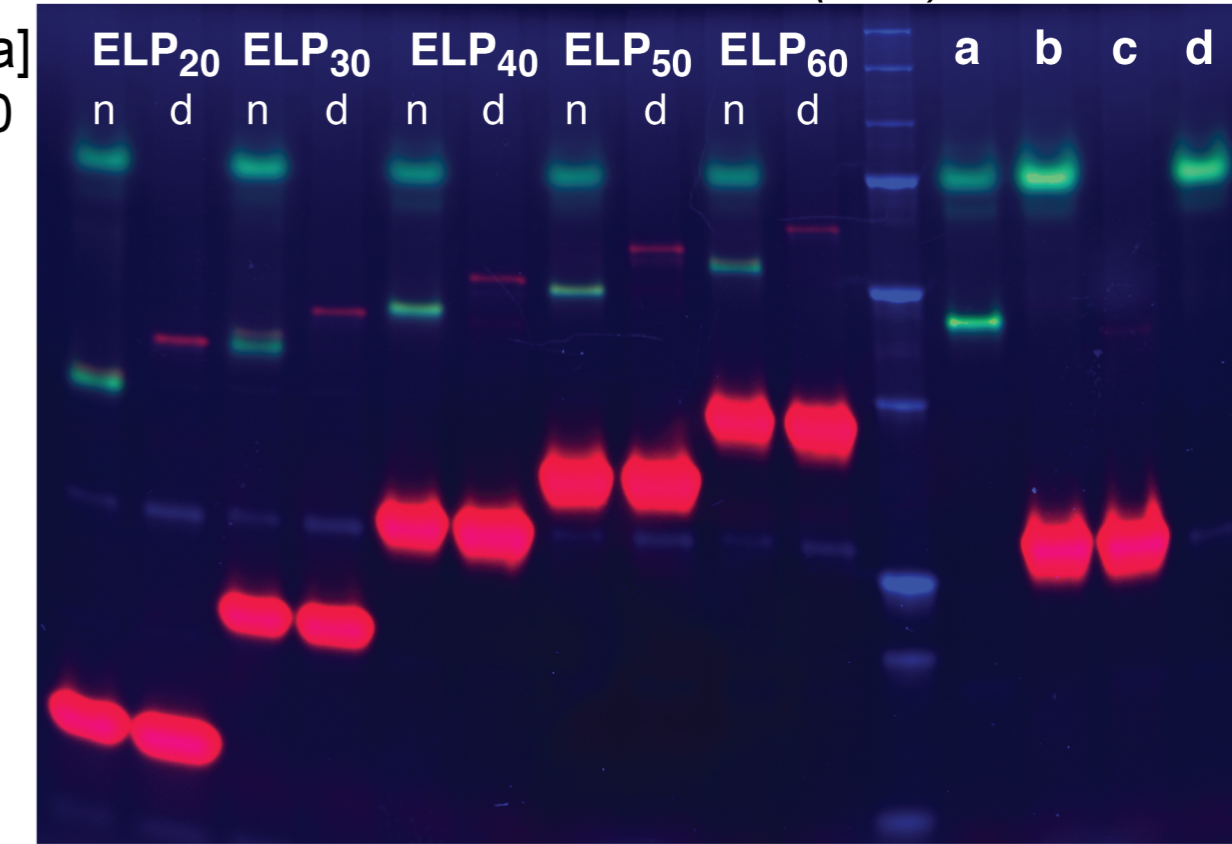
B Dye Fluorescence 530/28 - 695/55 nm



C GFP Fluorescence 470/30 - 530/28 nm



D Overlay: Panel B (red), Panel C (green) and UV Illumination (blue)



ELP₂₀₋₆₀: 20 - 60x Pentapeptide-Repeat
n: native **d**: denatured

a) ELP₄₀ + GFP + Sortase **b)** ELP₄₀ + GFP + Sfp

c) ELP₄₀ + Sfp + Sortase **d)** GFP + Sfp + Sortase

